Hindawi Publishing Corporation
Journal of Nanotechnology
Volume 2011, Article ID 904629, 9 pages
doi:10.1155/2011/904629

Research Article

Photocatalytic Degradation of Phenol Using Immobilized TiO_2 Nanotube Photocatalysts

Chung Leng Wong, Yong Nian Tan, and Abdul Rahman Mohamed

School of Chemical Engineering, Universiti Sains Malaysia, Engineering Campus, Nibong Tebal, Seberang Perai, Pulau, Pinang 14300, Malaysia

Correspondence should be addressed to Abdul Rahman Mohamed, chrahman@eng.usm.my

Received 16 March 2011; Revised 11 April 2011; Accepted 15 April 2011

Academic Editor: Andrei Kolmakov

TiO_2 nanotubes immobilized on silica gel were used in the photocatalytic degradation of phenol in a batch reactor. The highest rate of photocatalytic activity was observed when the ratios of TiO_2 nanotubes: silica gel: colloidal silica were 3 : 2 : 20. The optimal air flow rate for phenol degradation was 0.3 L/min while pH 3 was optimal for the reaction medium. Decreasing the initial phenol concentration led to an increase in phenol degradation efficiency due to more hydroxyl radicals being presented on the catalyst surface. Immobilized TiO_2 nanotubes showed higher photocatalytic activity than that of the pure TiO_2 which only achieved 87% degradation. Compared with pure TiO_2, the immobilized TiO_2 nanotubes benefited from a larger specific surface area and a low recombination rate of photogenerated electron-hole pairs. After three operating cycles, the decrease in photocatalytic activity of the immobilized TiO_2 nanotubes was slight, indicating that the immobilized TiO_2 nanotubes have excellent stability and reusability.

1. Introduction

Phenol and its derivatives, which are widely used in many industries such as the chemical, coal tar, herbicide, petrochemical, petroleum, pharmaceutical, and plastic industries, are often released in wastewater without any further treatment [1, 2]. Phenol is highly toxic and carcinogenic; it is resistant to degradation by many conventional biological treatments or chemical adsorption processes [1]. Commonly employed approaches are often ineffective because they merely transfer the organic pollutants from water to another medium without degrading or mineralizing the organic pollutants. In recent years, heterogeneous photocatalysis, one of the measures employed in modern advanced oxidation processes (AOPs), has been used to remove or mineralize a wide range of organic pollutants. With this approach, harmful organics are broken down in the presence of a catalyst and ultraviolet (UV) irradiation without generating secondary harmful pollutants [3]. In this regard, titanium dioxide (TiO_2) semiconductors have demonstrated various advantages in heterogeneous photocatalysis [4]. These favourable characteristics include biological and chemical inertness [5, 6], nontoxicity [5–7], strong oxidizing power [5, 6], availability [7], transparency, [8] and, at the molecular level, a wide band gap [9]. Nevertheless, significant improvements to TiO_2 semiconductor photocatalysts are essential before they can be adopted for wider usage [5, 10, 11].

In the 1990s, the discovery of carbon nanotubes by Iijima opened new fields in the material science sector [4]. Nanotubular materials are considered important in photocatalysis owing to their special electronic and mechanical properties, high photocatalytic activity, large specific surface area, and high pore volume [12, 13]. Several studies have shown that TiO_2 nanotubes have better physical and chemical properties in photocatalysis compared with other forms of titanium dioxide. TiO_2 nanotubes, with their larger specific surface area, pore volume, and high photocatalytic activity, have attracted a lot of attention [10].

Many approaches are available to synthesize TiO_2 nanotubes. These include chemical vapour deposition (CVD), anodic oxidation, seeded growth, and wet chemical (hydrothermal and sol-gel method) [14–16]. Among these approaches, the hydrothermal method is often chosen because of its many advantages such as cost-effectiveness,

low energy consumption, mild reaction condition, and simple equipment requirement [15]. The production of TiO_2 nanotubes through hydrothermal synthesis in absence of molds for template and replication was first reported by Kasuga et al. [17]. TiO_2 nanotubes of uniform diameter and specific surface area and length have been produced by this simple technique [10, 18]. The wide pore size distribution and high aspect ratio of TiO_2 nanotubes thus prepared are attractive candidates for photocatalysis.

However, the main drawback for its wider practical application is the limitation on mass transfer despite its large surface area. Recovery of ultrafine TiO_2 nanotubes for reuse by a filtration process is both tedious and costly. It also requires complex operations while the separation process does not guarantee complete recovery of the ultrafine tube-like structures [4, 19, 20]. Hence, current research activities are turning to the area of photocatalysis using the catalyst in an immobilized system. Various supports (glass beads, silica gel, quartz sand, etc.) are frequently used in the immobilization process due to the ease of suspension by air bubbling or mechanical stirring. Among these supports, silica gel is an excellent choice because of its high adsorption capacity and relatively low cost. Colloidal silica is used as a binder in the mixture of silica gel and immobilized TiO_2 nanotubes.

Although many experimental studies have assessed the photocatalytic degradation of organic pollutants using suspended TiO_2 nanotubes, few have focused on the use of immobilized TiO_2 nanotubes. This study was aimed at optimizing the components of an immobilized TiO_2 nanotube system used in degrading organic pollutants. The selection of the best catalyst, support and binder was made with the objective of minimizing wastage and costs. The effects of the operating parameters (air flow rate, medium pH, and initial phenol concentration) on the phenol degradation efficiency in a batch reactor were also investigated.

2. Experimental Procedure

2.1. Reagents. All chemicals were reagent grade and used without any further purification. Titanium (IV) oxide and silica gel (0.2–0.5 mm) used as the support for the TiO_2 nanotubes were purchased from Acros Organic. Sodium hydroxide pellet and fuming hydrochloric acid were purchased from Merck while colloidal silica (30 wt% silica suspension in water) and phenol (≥ 99.999%) were purchased from Sigma Aldrich. All the solutions were prepared using deionized water (18.2 Ω resistivity) from a Milli-Q system.

2.2. Preparation of TiO_2 Nanotubes/Silica Gel Photocatalyst. TiO_2 nanotubes were produced using a hydrothermal treatment based on Kasuga et al. [17], and as proposed by Lee et al. [6, 21]. One gram of titanium (IV) oxide was dissolved in each 25 mL aliquot of 10 M sodium hydroxide solution in a 200 mL Teflon liner receptacle. After stirring vigorously for 15 minutes, the white, milky suspensions were then autoclaved at 130°C for 3 h. After cooling to room temperature, the resulting products were filtered and washed repeatedly with 0.1 M hydrochloric acid and then with deionized water until approximately pH 7. The final precipitates were dried in the oven at 80°C.

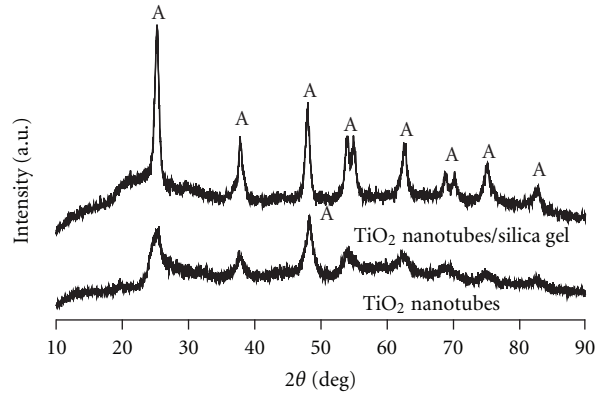

A: Anatase phase

Figure 1: XRD patterns of TiO_2 nanotubes/silica gel and TiO_2.

Silica gel used as the support was pretreated with acetone to remove organic matter. The silica gel was then rinsed with deionized water and dried in the oven at 80°C for 12 h. For the immobilization process, a known weight of TiO_2 nanotubes and silica gel were mixed in an appropriate amount of colloidal silica. After stirring for 15 min, the mixture was dried at room temperature for two days. Subsequently, it was dried in the oven at 100°C for 3 h. The final product was gently crushed and calcined at 600°C for 3 h using a multisegment, programmable, high-temperature furnace (Carbolite, UK).

2.3. Catalyst Characterization. The Brunauer-Emmett-Teller (BET) surface area of TiO_2 nanotubes/silica gel, TiO_2 nanotubes, pure TiO_2, and silica gel were 465, 359, 53, and 582 m^2/g, respectively. Hence, TiO_2 nanotubes had a relatively higher surface area compared with the pure TiO_2. The surface area of TiO_2 nanotubes was further enhanced after immobilization on silica gel. The surface area of TiO_2 nanotubes/silica gel was smaller than that of the silica gel, indicating that a portion of the TiO_2 nanotubes might have deposited inside the pores of silica gel. X-ray diffraction (XRD) analysis was used to examine the changes of crystalline phase and crystalline size of the TiO_2 nanotubes supported on silica gel. All the diffraction peaks of the samples (Figure 1) were anatase, and the average crystalline size calculated from diffraction peak broadening by the Scherer's formula was 23.14 nm. The SEM images (Figure 2(a)) of TiO_2 nanotubes/silica gel showed that TiO_2 nanotubes were immobilized well on the silica gel; some of them were agglomerated on the surface of silica gel. One of the advantages of using TiO_2 nanotubes/silica gel in the photocatalytic degradation of phenol is that the structure of TiO_2 nanotubes is maintained after the photocatalytic degradation reaction (Figure 2(b)).

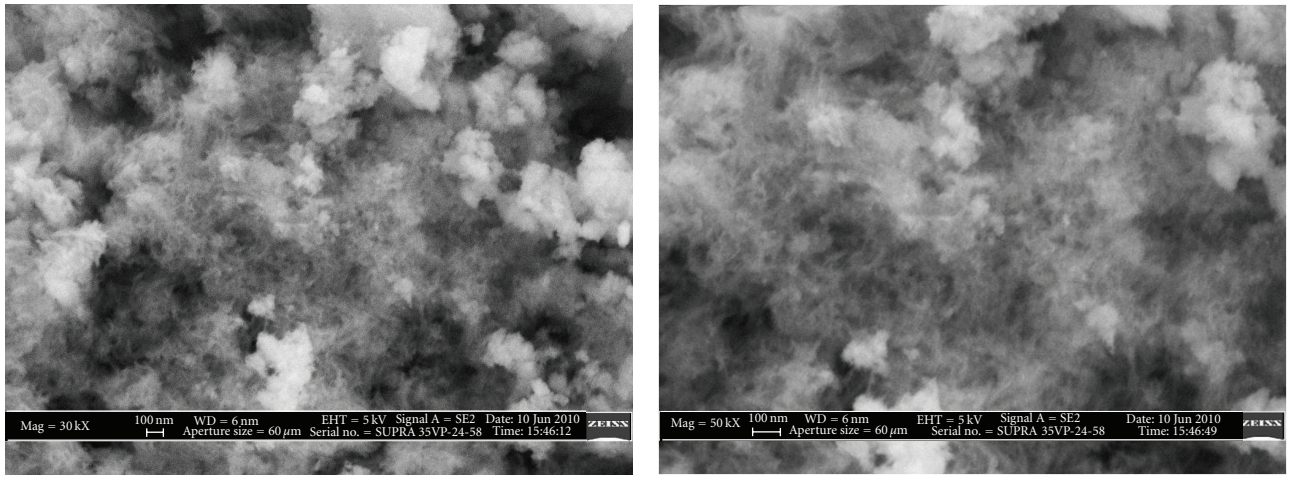

(a) (b)

Figure 2: SEM images of TiO_2 nanotubes/silica gel synthesized by the hydrothermal reaction at 130°C for 3 h. (a) Before photocatalytic degradation of phenol and (b) after photocatalytic degradation of phenol.

2.4. Photocatalytic Degradation Experiment. The photocatalytic activities of the prepared catalysts in degrading phenol were evaluated using a batch reactor, as shown in Figure 3 [22]. The batch reactor was equipped with a cylindrical Pyrex glass jacketed reactor which measured 23 cm × 10 cm × 8 cm (height × outer diameter × inner diameter) and with a total volume of 600 mL; this was used as the main chamber for the photocatalytic process. Pyrex glass was chosen because of its ability to control UV light (below 300 nm), thus preventing the photolysis of the organic compounds. The photocatalytic degradation process was conducted inside an enclosed black box to prevent any entry of stray light into the reactor. The phenol solutions were illuminated by a 15 W low-pressure mercury lamp (254 nm, PCQ lamp, UVP, Inc.) located in the center of the reactor to provide illumination for the photocatalytic reaction. A 1 cm diameter quartz tube was used to protect the lamp from direct contact with the phenol solution. The reactor was surrounded with a cooling jacket and a fan to control the temperature of the process and to protect the lamp from overheating. An air flow meter was located at the top of the reactor to measure and control air flow rate through the distributor. The solution was stirred continuously using a magnetic stirrer to ensure efficient mixing of the photocatalysts and phenol solution. The thermocouple was located at the top of the reactor to monitor temperature variations during the reaction. The sample port was located at the top of the reactor.

Phenol solution (500 mL) and 1 g/L of photocatalyst were fed into the reactor. The medium pH was adjusted using 0.1 M HCl or NaOH throughout the experiments. The air flow rate was adjusted using a rotameter. All the experiments were carried out at an ambient temperature (27 ± 2°C) and atmospheric pressure. An aqueous suspension of phenol containing the required quantity of photocatalysts was sonicated for 15 min, followed by premixing in the dark for 30 min to reach the adsorption/desorption equilibrium. The first sample was taken at the end of the dark run to determine the concentration of phenol solution (nonadsorbed). After that, the UV lamp was switched on to initiate the photocatalytic degradation reaction. During the experiments, air was bubbled into the phenol solutions at a constant flow rate. At 15-minute intervals for 120 min, 5 mL samples were drawn out of the reactor to determine the change of the phenol concentration after phenol degradation during UV irradiation.

The samples were centrifuged and filtered using WHATMAN filter (PTFE-membrane, 0.20 μm) to remove the suspended solids. The photocatalytic degradation of phenol was measured by high-performance liquid chromatography (HPLC, Perkin Elmer 275) and the photocatalytic degradation efficiency was determined using the following formula.

$$\text{Photocatalytic degradation efficiency} = \left(\frac{C_i}{C_0}\right), \quad (1)$$

where C_i was the concentration of phenol at time t and C_0 was the initial concentration of phenol.

3. Results and Discussion

3.1. Identification Factors Influencing the Photocatalytic Activity. The photocatalytic degradation of phenol was initially studied under three different experimental conditions: (1) in darkness, in the absence of catalyst, (2) in darkness, in the presence of catalyst (adsorption), and (3) with UV irradiation, in the absence of catalyst (photolysis). The concentration of phenol in each experiment was 30 mg/L, and the experiments were carried out under the following conditions: catalyst comprising TiO_2 nanotubes, silica gel, and colloidal silica in the ratios of 3 : 2 : 20; catalyst loading of 1 g/L, medium pH 3 and air flow rate of 0.3 L/min. In the preliminary experiments, reactants were premixed in the dark for 30 min and irradiated with UV light for 120 min. For (1) and (2), the experiments were operated in the absence of UV light for 120 min after the 30 min of the dark run.

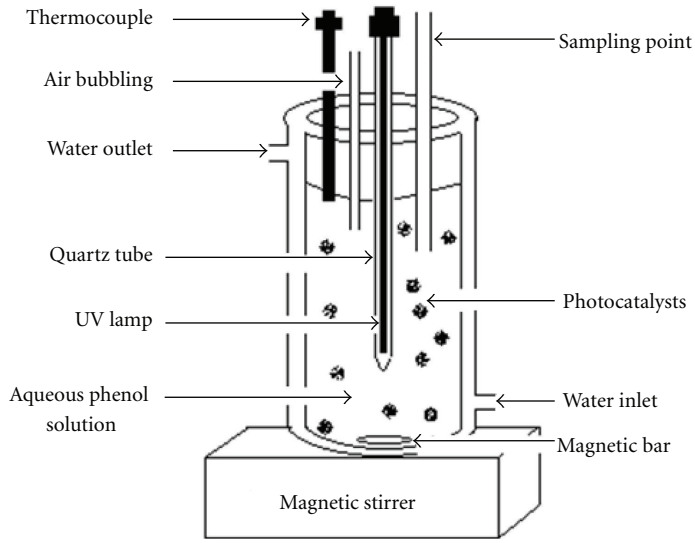

Figure 3: A schematic diagram of batch reactor.

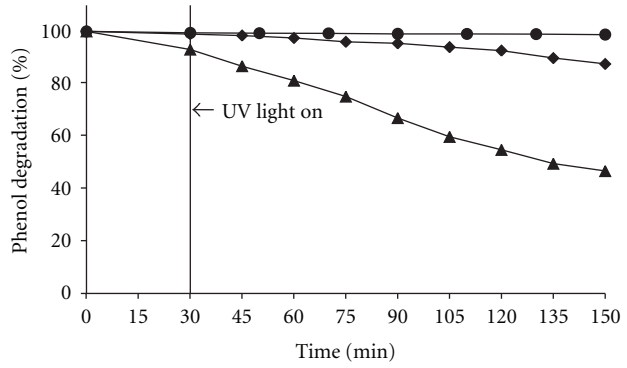

Figure 4: Photocatalytic degradation of phenol under different conditions. Conditions: catalyst comprised TiO_2 nanotubes, silica gel, and colloidal silica in the ratio of 3 : 2 : 20; catalyst loading = 1 g/L, air flow rate = 0.3 L/min, and initial phenol concentration = 30 mg/L. (• = in darkness, in the absence of the catalyst, ▲ = in darkness, in the presence of the catalyst, and ♦ = UV irradiation in the absence of the catalyst).

The results in Figure 4 show that about 1.9% degradation was observed in darkness after 150 min, indicating an insignificant adsorption of phenol onto the quartz glass column. Only 12.4% degradation was achieved when the phenol solution was irradiated with UV light for 150 min, in the absence of the photocatalyst. A greater degradation of phenol (53.3%) was recorded in darkness, but in the presence of the photocatalyst. This reaction was due to phenol adsorption onto the prepared photocatalysts, but it was not a light-driven reaction since it occurred in darkness.

3.2. Optimal Composition of TiO_2 Nanotubes/Silica Gel Photocatalyst for the Photocatalytic Degradation of Phenol. The selection of the optimum composition (catalyst, support, and binder) was aimed at maximizing performance and minimizing cost. Hence, the effect of each component in the photocatalysis system was investigated using the photocatalytic degradation of phenol in a batch reactor as a model.

3.2.1. TiO_2 Nanotubes Loading. To study the effect of TiO_2 nanotubes loading on the rate of photocatalytic degradation of phenol solution, TiO_2 nanotubes loading was varied in the range of 0.04–0.16 g/L. The results in Figure 5 show that the phenol degradation activity increased when loading in TiO_2 nanotubes was raised. This is in agreement with the finding of Zainudin et al. [23]. The photocatalytic degradation reaction normally takes place on the TiO_2 nanotubes surface [23]. Possible reasons for the increased photocatalytic degradation performance are (1) the increase in the number of active sites of TiO_2 nanotubes, (2) the presence of the photons absorbed leading to an increase in the number of phenol molecules adsorbed [22], and (3) the generation of positive holes and hydroxyl radicals in the reaction causing an increase in the number of surface active sites [1] as reported in the literature.

The results showed that the photocatalytic performance of 0.12 g/L TiO_2 nanotubes was not very different from that from using 0.16 g/L TiO_2 nanotubes. To maintain a high level of phenol degradation activity while avoiding any unnecessary excess of photocatalyst, 0.12 g/L TiO_2 nanotubes were chosen for optimal loading in the preparation of the immobilized TiO_2 nanotubes.

3.2.2. Silica Gel Loading. The influence of silica gel loading on the phenol degradation efficiency was studied at loadings varying from 0.04 g/L to 0.16 g/L. Figure 6 shows the phenol degradation efficiency for the degradation of phenol as a function of silica gel loading. In darkness, the adsorption of phenol on the TiO_2 nanotubes/silica gel increased with increasing silica gel content in the catalyst. Under UV irradiation, however, the silica gel loading of 0.08 g/L gave

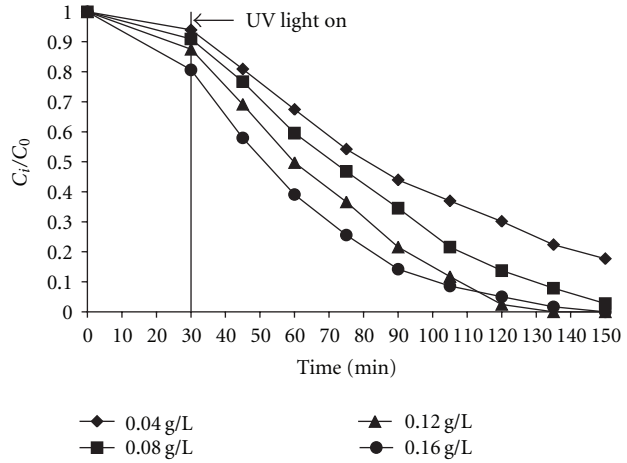

Figure 5: Effect of TiO_2 nanotubes loading on the phenol degradation. Conditions: silica gel and colloidal silica in the catalyst were 0.08 and 0.80 g/L, respectively, air flow rate = 0.3 L/min, initial phenol concentration = 30 mg/L and pH = 3.

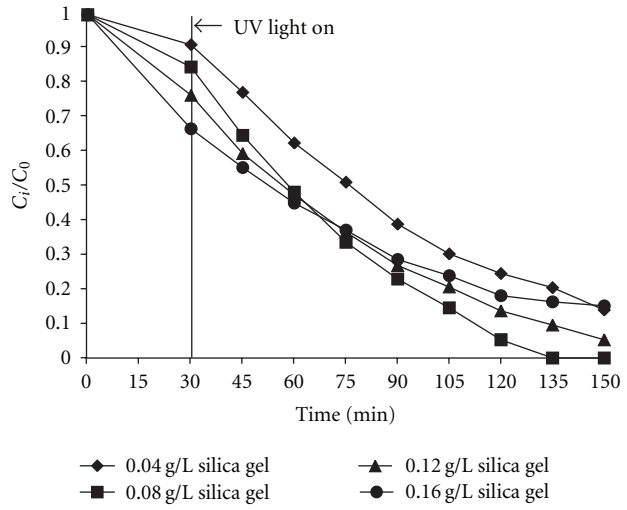

Figure 6: Photocatalytic performance of different silica gel loading in the phenol degradation. Conditions: TiO_2 nanotubes and colloidal silica in the catalyst were 0.12 and 0.80 g/L, respectively, air flow rate = 0.3 L/min, initial phenol concentration = 30 mg/L, and medium pH = 3.

the best result. Beyond this loading, the efficiency of phenol degradation decreased, perhaps due to the phenol adsorption ability of silica gel. This observation agrees with the earlier finding [22] showing that an increase in the adsorption ability of support decreased the photocatalytic degradation.

3.2.3. Binder Loading. According to Zainudin et al. [23], colloidal silica binder supports efficiency in the degradation of organic compounds. Immobilization of TiO_2 nanotubes onto silica gel was achieved by a simple binding method in this study. One advantage in immobilizing TiO_2 nanotubes onto silica gel is that it provides good adherence between the support and the catalyst over a sustained period without

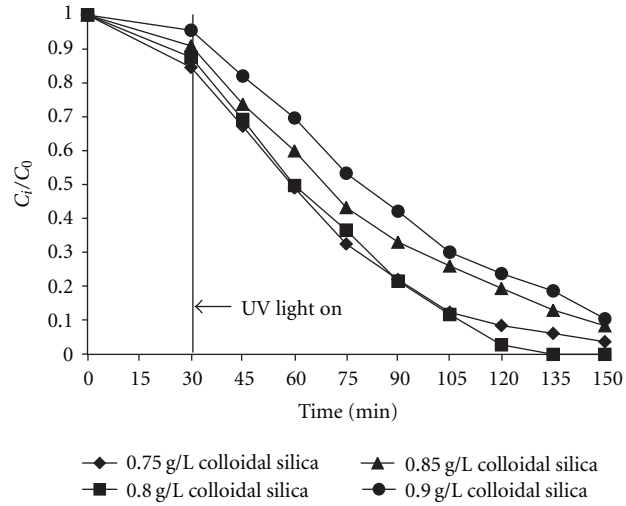

Figure 7: Photocatalytic degradation of aqueous phenol solution at different colloidal silica loading. Conditions: TiO_2 nanotubes and silica gel in the catalyst were 0.12 and 0.08 g/L, respectively, air flow rate = 0.3 L/min, initial phenol concentration = 30 mg/L, and medium pH = 3.

adversely affecting its photocatalytic function. The effect of the colloidal silica load on the efficiency of phenol photocatalytic degradation was assessed by varying the amount of the binder. The results in Figure 7 show that the degradation efficiency of phenol increased when the colloidal silica content was increased from 0.75 to 0.80 g/L. Further increase in colloidal silica amounts resulted in a decrease in the rate of phenol degradation.

Based on Sections 3.2.1–3.2.3, the optimum amount of TiO_2 nanotubes loading was found to be 0.12 g/L for the photocatalytic degradation of phenol, taking into the consideration both the phenol degradation efficiency and costs savings. Since the photocatalytic performance of 0.12 g/L TiO_2 nanotubes was not very different from 0.16 g/L TiO_2 nanotubes, the former loading was chosen to reduce the operational costs. The optimum loading of silica gel and colloidal silica were found to be 0.08 g/L and 0.80 g/L, respectively. Overall, the optimum composition of the photocatalyst comprising TiO_2 nanotubes, silica gel and colloidal silica was 3 : 2 : 20. In practical terms, 0.06 g TiO_2 nanotubes are required for the degradation of 500 mL phenol (0.12 g/L TiO_2 nanotubes).

3.3. Effect of Operating Parameters

3.3.1. Effect of Medium pH. The medium pH affects the surface charge for the photocatalyst, as well as the type of organic pollutants [24]. The effect of the variation of pH was studied on the photocatalytic degradation of phenol by adjusting with 0.1 M HCl and NaOH solutions.

After the illumination process, the medium changed from colorless to a shade of pink when the pH value decreased, as reported by Laoufi et al. [1]. With further increases in the illumination time, the medium changed back

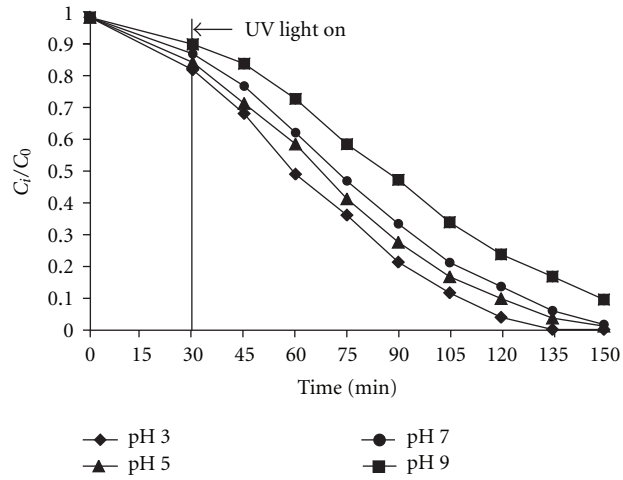

Figure 8: Effect of medium pH on the photocatalytic degradation of aqueous phenol solution. Conditions: catalyst comprised TiO_2 nanotubes, silica gel, and colloidal silica in the ratio of 3 : 2 : 20, air flow rate = 0.3 L/min and initial phenol concentration = 30 mg/L.

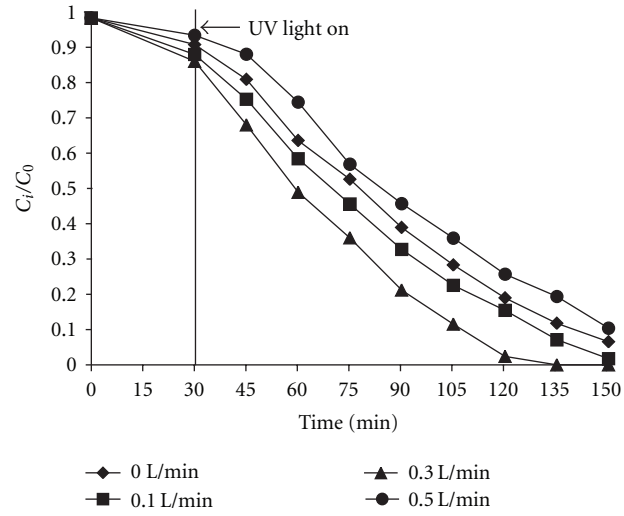

Figure 9: Influence of air flow rate on the photocatalytic degradation of aqueous phenol solution. Experimental conditions: catalyst comprised TiO_2 nanotubes, silica gel, and colloidal silica in the ratio of 3 : 2 : 20, medium pH = 3, and initial phenol concentration = 30 mg/L.

to being colorless. In this study, the degradation efficiency was highest at pH 3 whereas lower efficiencies were observed at pH 5, 7, and 9 (Figure 8).

Those efficiencies can be explained on the basis of the zero point charge of TiO_2 nanotubes [25]. The zero point charge is known as the pH value at which the concentration of protonated and deprotonated surface groups are equal [25]. The pH for the zero point charge (pzc) of TiO_2 nanotubes is 3 [26]. According to Lam et al. [27], the following equilibrium reactions operate:

$$\text{pH} < \text{pH}_{\text{pzc}} \quad \text{TiOH} + \text{H}^+ \longrightarrow \text{TiOH}_2{}^+ \tag{2}$$

$$\text{pH} > \text{pH}_{\text{pzc}} \quad \text{TiOH} + \text{OH}^- \longrightarrow \text{TiO}^- + \text{H}_2\text{O} \tag{3}$$

where TiOH is the titanol surface group.

In considering the negative charge of phenol (phenol^-) and the positive charge of the immobilized TiO_2 nanotubes surface (TiO_2 nanotubes/silica gel)$^+$ [28], the electrostatic adsorption exists when these phenol^- anions are more likely located at the positive sites [29]. As shown in Figure 8, the photocatalytic efficiencies are higher at acidic concentrations. Thus, the acidic medium is confirmed to have better degradation efficiency than the alkaline or neutral media. At pH 9, the electrostatic repulsion presents itself between the negative surface of the photocatalyst and the organic pollutants (phenol^-). On the other hand, the presence of the electrostatic repulsion also retards the adsorption, thus decreasing the phenol degradation efficiency [30].

3.3.2. Effect of Air Flow Rate. Air flow rate was controlled to enhance the rate of photocatalytic degradation of phenol in aqueous suspension of the immobilized TiO_2 nanotube itself. The air flow rate was varied between 0 to 0.5 L/min. The degradation of phenol (Figure 9) increased as the air flow rate rose until 0.3 L/min. Further increase in air flow rate beyond this value resulted in a decrease in phenol degradation rate. Better photocatalytic degradation in the initial stage of increasing the air flow rate was a consequence of an increased diffusion between phenol and immobilized TiO_2 nanotubes, resulting in higher mass transfer rate. An air flow rate greater than 0.3 L/min did not increase phenol degradation efficiency due to limitations of phenol adsorption ability on the surface of immobilized TiO_2 nanotubes. These observations agree with the earlier findings [27, 31] which showed that the air flow rate beyond a certain level would reduce the adsorption ability of phenol onto the photocatalyst surface, thus decreasing photocatalytic degradation in the process.

3.3.3. Effect of Initial Phenol Concentration. Figure 10 shows the effect of the initial phenol concentration on the photocatalytic degradation efficiency. The initial phenol concentration in this study was varied from 10 to 110 mg/L. The phenol degradation efficiency decreased as initial phenol concentration increased. A possible reason is that the generation of hydroxyl radicals on the catalyst surface is reduced when the initial phenol concentration is increased [30]. More phenol molecules are adsorbed on the surface of TiO_2 nanotubes/silica gel photocatalyst will make fewer active sites available for the hydroxyl radicals adsorption. Hence, large amounts of adsorbed phenol would have an inhibitory influence on the reaction between phenol molecules and hydroxyl radicals due to the lack of any direct contact between them. Once the phenol concentration is increased, most of UV light is absorbed by the phenol molecules [27], and photons do not reach the surface of photocatalyst to activate it to generate hydroxyl radicals.

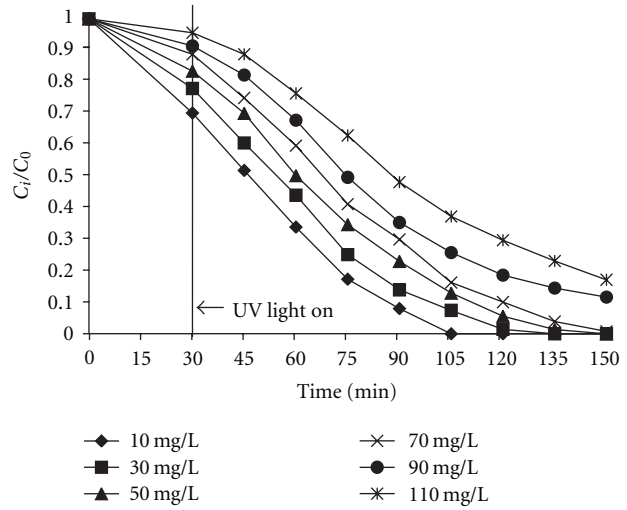

Figure 10: Effect of initial phenol concentration on the photocatalytic degradation efficiency. Experimental conditions: catalyst comprised TiO_2 nanotubes, silica gel, and colloidal silica in the ratio of 3 : 2 : 20, medium pH = 3, and air flow rate = 0.3 L/min.

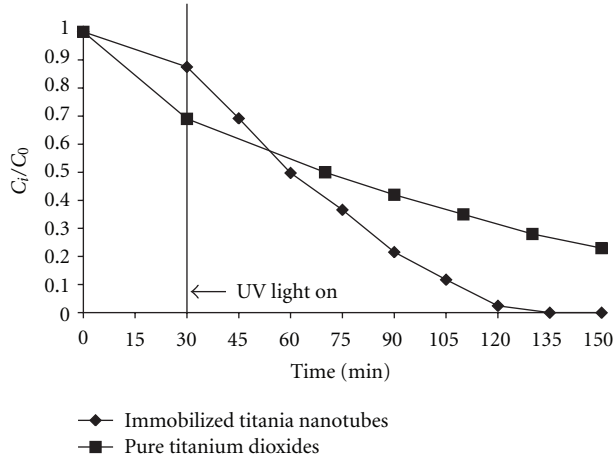

Figure 11: Photocatalytic activity of immobilized TiO_2 nanotubes and pure TiO_2. Conditions: air flow rate = 0.3 L/min, medium pH =3 and initial phenol concentration = 30 mg/L).

3.4. Comparison between Immobilized TiO_2 Nanotubes and Pure TiO_2. The photocatalytic activity of pure TiO_2 was analyzed in comparison with that of the immobilized TiO_2 nanotubes. As can be seen in Figure 11, the optimum composition of immobilized TiO_2 nanotubes (TiO_2 nanotubes : silica gel : colloidal silica = 3 : 2 : 20) shows the higher photocatalytic activity as compared with pure TiO_2. This finding agrees with several previous studies that showed TiO_2 nanotubes having better physical and chemical photocatalytic properties as compared with TiO_2 nanopowders. Colmenares et al. [32] reported that TiO_2 nanotubes had a relatively higher interfacial charge transfer rate and surface area compared with spherical TiO_2 particles. The immobilized TiO_2 nanotubes that comprised single anatase phase high crystalline TiO_2 nanotubes created an abundance of photogenerated electron-hole pairs with longer lifetimes. The transfer of the charge carriers along the length of TiO_2 nanotubes could minimize the recombination rate of photogenerated electron and positive hole. Li et al. [33] found that TiO_2 nanotubes were highly efficient in the photocatalytic degradation of methyl orange compared with the rutile phase TiO_2 nanopowders. The photocatalytic performance of the optimized TiO_2 nanotube composition achieved 100% of phenol degradation, whereas pure TiO_2 attained only 87% degradation. The results showing increased photocatalytic activity in Figure 11 would have been partly due to an increase in the specific surface area of the immobilized TiO_2 nanotubes (465 m^2/g) when compared with that of pure TiO_2 (53 m^2/g).

3.5. Photocatalytic Activity of the Recycled Immobilized TiO_2 Nanotubes. The long term serve life of immobilized TiO_2 nanotubes was studied by repeated photocatalytic degradation of an aqueous phenol solution with an initial phenol concentration of 30 mg/L, a medium pH of 3 and an air flow rate of 0.3 L/min. Once the photocatalytic degradation process was completed, the photocatalysts at the end of the first experimental run were recovered, washed with deionized water, and dried in an oven without any pretreatment. The photocatalysts were then utilized in a second cycle for the degradation of phenol with an initial concentration of 30 mg/L. A third experimental cycle was run under the same conditions.

The results for the degradation reaction using fresh immobilized TiO_2 nanotubes, and once or twice recycled immobilized TiO_2 nanotubes are shown in Figure 12. There were only very slight decreases in photocatalytic efficiencies of the immobilized TiO_2 nanotubes in the second and third cycles. The loss in percentage of photocatalytic degradation was less than 1% even after the third cycle (Figure 12). After each experimental run, the originally white color of the immobilized TiO_2 nanotubes was observed to turn light yellow. This might be due to the blocking of active sites by some phenol intermediates such as catechol, hydroquinone, p-benzoquinone, and resorcinol [2, 23], thus decreasing the photocatalytic activity of the immobilized TiO_2 nanotubes.

Colloidal silica provides good adherence between TiO_2 nanotubes and the silica gel. This confers high stability to the photocatalyst and leads to its good performance over a prolonged period. TiO_2 nanotubes/silica gel are very stable since they do not dissolve into the medium [27]. After three cycles of repeated use, the structure of TiO_2 nanotubes (Figure 2(b)) in TiO_2 nanotubes/silica gel photocatalysts in the present study was well preserved, and the decline in photocatalytic degradation efficiency was only slight (Figure 12).

4. Conclusion

To investigate the photocatalytic degradation of phenol in the presence of TiO_2 nanotubes/silica gel photocatalysts, TiO_2 nanotubes/silica gel photocatalysts were prepared by hydrothermal treatment and a simple binding method. The

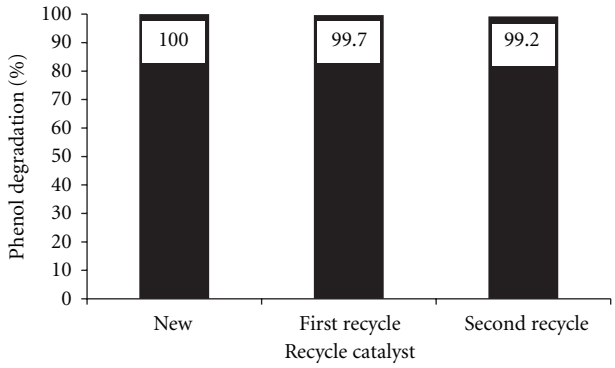

Figure 12: Effect of catalyst recycling on the photocatalytic degradation of phenol under 120 min of irradiation duration (air flow rate = 0.3 L/min, initial phenol concentration = 30 mg/L, and pH = 3).

effects of TiO_2 nanotubes loading, silica gel loading, and colloidal silica loading were found to be 3 : 2 : 20, and photocatalysts prepared accordingly performed very well in the photocatalytic degradation of phenol. High photocatalytic efficiency was observed with a medium pH of 3 and an air flow rate of 0.3 L/min. The photocatalytic degradation of phenol performed best at low initial phenol concentration as the photocatalytic degradation efficiency decreased with increasing initial phenol concentration. Phenol was completely degraded using immobilized TiO_2 nanotubes whereas only 87% degradation was achieved using pure TiO_2. After three cycles of usage, the photocatalysts suffered only a slight decrease in performance, showing that immobilized TiO_2 nanotubes have excellent stability and reusability.

Acknowledgments

The authors would like to acknowledge the funding support received from Universiti Sains Malaysia (USM) through the USM Fellowship, Fundamental Research Grant Scheme (FRGS; 1001/PJKIMIA/811068) and through the Postgraduate Research Grant Scheme (1001/PJKIMIA/8033054).

References

[1] N. A. Laoufi, D. Tassalit, and F. Bentahar, "The degradation of phenol in water solution by TiO_2 photocatalysis in a helical reactor," *Global NEST Journal*, vol. 10, pp. 404–418, 2008.

[2] K. Okamoto, Y. Yanamoto, H. Tanaka, M. Tanaka, and A. Itaya, "Heterogeneous photocatalytic decomposition of phenol over TiO_2 poweder," *Bulletin of the Chemical Society of Japan*, vol. 58, pp. 2015–2022, 1985.

[3] S. Funda, E. Sema, A. Meltem et al., "Photocatalytic performance of pure anatase nanocrystallite TiO_2 synthesized under low temperature hydrothermal conditions," *Materials Research Bulletin*, vol. 41, no. 12, pp. 2276–2285, 2006.

[4] L. L. Costa and A. G. S. Prado, "TiO_2 nanotubes as recyclable catalyst for efficient photocatalytic degradation of indigo carmine dye," *Journal of Photochemistry and Photobiology A*, vol. 201, no. 1, pp. 45–49, 2009.

[5] J. G. Yu, H. G. Yu, B. Cheng, and C. Trapalis, "Effects of calcination temperature on the microstructures and photocatalytic activity of titanate nanotubes," *Journal of Molecular Catalysis A*, vol. 249, no. 1-2, pp. 135–142, 2006.

[6] C. K. Lee, M. D. Lyu, S. S. Liu, and H. C. Chen, "The synthetic parameters for the preparation of nanotubular titanate with highly photocatalytic activity," *Journal of the Taiwan Institute of Chemical Engineers*, vol. 40, no. 4, pp. 463–470, 2009.

[7] S. Sreekantan and L. C. Wei, "Study on the formation and photocatalytic activity of titanate nanotubes synthesized via hydrothermal method," *Journal of Alloys and Compounds*, vol. 490, no. 1-2, pp. 436–442, 2010.

[8] V. E. Nawin, S. Noriaki, C. Tawatchai, K. Takeyuki, and T. Wiwut, "A step towards length control of titanate nanotubes using hydrothermal reaction with sonication pretreatment," *Nanotechnology*, vol. 19, pp. 1–6, 2008.

[9] B. X. Wang, D. F. Xue, Y. Shi, and F. H. Xue, "Titania 1D nanostructured materials: synthesis, properties, and applications," in *Nanorods, Nanotubes and Nanomaterials Research Progress*, W. V. Prescott and A. I. Schwartz, Eds., New Nova Science, New York, NY, USA, 2008.

[10] H. G. Yu, J. G. Yu, B. Cheng, and J. Lin, "Synthesis, characterization and photocatalytic activity of mesoporous titania nanorod/titanate nanotube composites," *Journal of Hazardous Materials*, vol. 147, no. 1-2, pp. 581–587, 2007.

[11] C. K. Lee, H. C. Chen, S. S. Liu, and F. C. Huang, "Effect of sodium content and calcination temperature on the morphology, structure and photocatalytic activity of nanotubular titanates," *Journal of the Taiwan Institute of Chemical Engineers*, vol. 41, pp. 373–380, 2010.

[12] V. Idakiev, Z. Y. Yuan, T. Tabakova, and B. L. Su, "Titanium oxide nanotubes as supports of nano-sized gold catalysts for low temperature water-gas shift reaction," *Applied Catalysis A*, vol. 281, no. 1-2, pp. 149–155, 2005.

[13] J. G. Yu and H. G. Yu, "Facile synthesis and characterization of novel nanocomposites of titanate nanotubes and rutile nanocrystals," *Materials Chemistry and Physics*, vol. 100, no. 2-3, pp. 507–512, 2006.

[14] D. L. Morgan, H. Y. Zhu, R. L. Forst, and E. R. Waclawik, "Determination of a morphological phase diagram of titania/titanate nanostructures from alkaline hydrothermal treatment of Degussa P25," *Chemistry of Materials*, vol. 20, no. 12, pp. 3800–3802, 2008.

[15] Y. P. Guo, N. H. Lee, H. J. Oh et al., "Preparation of titanate nanotube thin film using hydrothermal method," *Thin Solid Films*, vol. 516, no. 23, pp. 8363–8371, 2008.

[16] F. M. Wang, Z. S. Shi, F. Gong, J. T. Jiu, and M. Adachi, "Morphology control of anatase TiO_2 by surfactant-assisted hydrothermal method," *Chinese Journal of Chemical Engineering*, vol. 15, no. 5, pp. 754–759, 2007.

[17] T. Kasuga, M. Hiramatsu, A. Hoson, T. Sekino, and K. Niihara, "Formation of titanium oxide nanotube," *Langmuir*, vol. 14, no. 12, pp. 3160–3163, 1998.

[18] Y. Okour, H. K. Shon, I. J. E. Saliby, R. Naidu, J. B. Kim, and J. H. Kim, "Preparation and characterization of titanium dioxide (TiO_2) and thiourea-doped titanate nanotubes prepared from wastewater flocculated sludge," *Bioresource Technology*, vol. 101, pp. 1453–1458, 2009.

[19] S. Ribbens, V. Meynen, G. V. Tendeloo et al., "Development of photocatalytic efficient Ti-based nanotubes and nanoribbons by conventional and microwave assisted synthesis strategies," *Microporous and Mesoporous Materials*, vol. 114, pp. 401–409, 2008.

[20] A. K. Gupta, A. Pal, and C. Sahoo, "Photocatalytic degradation of a mixture of crystal violet (basic violet 3) and methyl red dye in aqueous suspensions using Ag^+ doped TiO_2," *Dyes and Pigments*, vol. 69, no. 3, pp. 224–232, 2006.

[21] C. K. Lee, K. S. Lin, C. F. Wu, M. D. Lyu, and C. C. Lo, "Effects of synthesis temperature on the microstructures and basic dyes adsorption of titanate nanotubes," *Journal of Hazardous Materials*, vol. 150, no. 3, pp. 494–503, 2008.

[22] N. F. Zainudin, A. Z. Abdullah, and A. R. Mohamed, "Characteristics of supported nano-TiO_2/ZSM-5/silica gel (SNTZS): photocatalytic degradation of phenol," *Journal of Hazardous Materials*, vol. 174, pp. 299–306, 2010.

[23] N. F. Zainudin, A. Z. Abdullah, and A. R. Mohamed, "Development of supported TiO_2 photocatalyst based adsorbent for photocatalytic degradation of phenol," in *Proceedings of the International Conference on Environment (ICENV '08)*, Penang, Malaysia, 2008.

[24] P. R. Gogate and A. B. Pandit, "A review of imperative technologies for wastewater treatment I: oxidation technologies at ambient conditions," *Advances in Environmental Research*, vol. 8, no. 3-4, pp. 501–551, 2004.

[25] G. M. Madhu, M. A. L. A. Raj, K. V. K. Pai, and S. Rao, "Photodegradation of methylene blue dye using UV/$BaTiO_3$, UV/H_2O_2 and UV/H_2O_2/$BaTiO_3$ oxidation processess," *Indian Journal of Chemical Technology*, vol. 14, no. 2, pp. 139–144, 2007.

[26] D. V. Bavykin, E. V. Milsom, F. Marken et al., "A novel cation-binding TiO_2 nanotube substrate for electro- and bioelectrocatalysis," *Electrochemistry Communications*, vol. 7, no. 10, pp. 1050–1058, 2005.

[27] S. M. Lam, J. C. Sin, and A. R. Mohamed, "Parameter effect on photocatalytic degradation of phenol using TiO_2-P25/activated carbon (AC)," *Korean Journal of Chemical Engineering*, vol. 27, no. 4, pp. 1109–1116, 2010.

[28] Y. X. Chen, K. Wang, and L. P. Lou, "Photodegradation of dye pollutants on silica gel supported TiO_2 particles under visible light irradiation," *Journal of Photochemistry and Photobiology A*, vol. 163, no. 1-2, pp. 281–287, 2004.

[29] N. M. Mahmoodi and M. Arami, "Degradation and toxicity reduction of textile wastewater using immobilized titania nanophotocatalysis," *Journal of Photochemistry and Photobiology B*, vol. 94, no. 1, pp. 20–24, 2009.

[30] N. Daneshvar, D. Salari, A. Niaei, M. H. Rasoulifard, and A. R. Khataee, "Immobilization of TiO_2 nanopowder on glass beads for the photocatalytic decolorization of an azo dye C.I. direct red 23," *Journal of Environmental Science and Health*, vol. 40, no. 8, pp. 1605–1617, 2005.

[31] H. L. Yu, K. L. Zhang, and C. Rossi, "Theoretical study on photocatalytic oxidation of VOCs using nano-TiO_2 photocatalyst," *Journal of Photochemistry and Photobiology A*, vol. 188, no. 1, pp. 65–73, 2007.

[32] J. C. Colmenares, R. Luque, J. M. Campelo, F. Colmenares, Z. Karpinski, and A. A. Romero, "Nanostructured photocatalysts and their applications in the photocatalytic transformation of lignocellulosic biomass: an overview," *Materials*, vol. 2, pp. 2228–2258, 2009.

[33] H. L. Li, W. L. Luo, W. Y. Tian et al., "Fabrication and photocatalytic activity of Pt-inserted titania nanotubes," *Guang Pu Xue Yu Guang Pu Fen Xi*, vol. 29, no. 6, pp. 1623–1626, 2009.